LOW-PROFILE MULTIBRANCH MONOPOLE ANTENNA WITH INTEGRATED MATCHING CIRCUIT FOR LTE/WWAN/WLAN OPERATION IN THE TABLET COMPUTER

Po-Wei Lin and Kin-Lu Wong
Department of Electrical Engineering, National Sun Yat-sen University, Kaohsiung 80424, Taiwan, Republic of China; Corresponding author: wongkl@ema.ee.nsysu.edu.tw

Received 12 November 2013

ABSTRACT: *A low profile, small-size, planar tablet computer antenna for the long-term evolution (LTE)/wireless wide area network and 2.4-GHz WLAN operation is presented. The antenna is formed by three monopole strips configured into a compact configuration and printed on a thin FR4 substrate of size 10 × 40 mm^2. A high-pass matching circuit is integrated thereon, without increasing the antenna size, to greatly enhance the antenna's low-band bandwidth to cover the LTE700/GSM850/900 operation (704–960 MHz) with a low-antenna profile of 10 mm. The antenna's higher band is formed by two wide resonant modes contributed by the monopole strips and can cover the GSM1800/1900/UMTS/LTE2300/2500 operation (1710–2170/2300–2400/2500–2690 MHz). In addition, one of the resonant modes in the higher band can be adjusted to occur at about 2.4 GHz such that enhanced radiation characteristics for frequencies in the 2400–2484-MHz WLAN band are obtained for the proposed antenna.* Microwave Opt Technol Lett 56:1662–1666, 2014; View this article online at wileyonlinelibrary.com. DOI 10.1002/mop.28404

Key words: *mobile antennas; small antennas; long-term evolution/wireless wide area network/WLAN antennas; tablet computer antennas; antennas with integrated matching circuit*

1. INTRODUCTION

To achieve multiband operations for the internal mobile device antennas, the use of multiple radiating strips or resonators to generate multiple resonant modes has been known to be a useful technique. However, for operating in the WWAN (wireless wide area network) and/or long-term evolution (LTE) operation, the use of multiple radiating strips may lead to large or bulky antenna volume required for the internal antennas to be embedded in the mobile devices such as the tablet computers and laptop computers. As an example, an inverted-F antenna with multiple radiating strips that has been reported to cover multiband LTE/WWAN operation in a laptop computer requires a large area of 96 × 11.2 mm^2 [1], although the antenna has an attractive planar structure for slim laptop computer applications. The large occupied area for the antenna may cause problems in embedding two such antennas inside the mobile devices for multiinput multioutput (MIMO) or diversity operation [2].

Many related LTE/WWAN antennas suitable for laptop computer or tablet computer applications have also been reported [3–13]. The design techniques applied in these antennas include using multiple strip resonators [3–9], or multiple slot resonators [10], or comprising loop resonators [11–13]. Among these reported LTE/WWAN antennas, only few of them are with a planar structure suitable for slim laptop computer or tablet computer applications [1,7–9,13], in which the antenna's metal patterns occupy an area on a dielectric substrate from about 96 × 11.2 mm^2 [1] to 45 × 10 mm^2 [9].

In this article, based on the use of multiple strip resonators, we present a promising antenna configuration with small size and planar structure for the LTE/WWAN and 2.4-GHz WLAN operation (704–960/1710–2690 MHz bands) in the tablet computers. The antenna is formed by three monopole strips configured into a compact configuration and printed on a thin FR4 substrate of small size 10 × 40 mm^2 for achieving the LTE/WWAN/WLAN operation. The multiband/wideband operation with a small-antenna size is aided by an integrated matching circuit on the FR4 substrate, without increasing the antenna size. In addition to the acceptable LTE/WWAN operation obtained for the antenna, one of the three monopole strips can be easily adjusted to generate a resonant mode thereof at about 2.4 GHz such that enhanced radiation performances in the 2400–2484-MHz WLAN band can also be achieved. Details of the proposed antenna are presented.

2. PROPOSED ANTENNA AND PARAMETRIC STUDY

Figure 1 shows the proposed LTE/WWAN/WLAN tablet computer antenna. An equivalent circuit of the integrated matching circuit and the three monopole strips in the antenna is also provided in the figure. A photo of the fabricated antenna is shown in Figure 2. The antenna is printed on a 0.8-mm thick FR4 substrate of size 10 × 40 mm^2, relative permittivity 4.4, and loss tangent 0.024. The antenna is mounted along an edge and at a corner of the device ground plane of dimensions 150 × 200 mm^2. In the experiment, the device ground plane was cut from a 0.2-mm thick copper plate (see the photo inset in Fig. 7). It is also noted that the selected dimensions of the device ground plane are reasonable for a practical tablet computer with a 9.7-inch display panel. The antenna's feeding point and grounding point are at Point A and B, and for testing the antenna, a 50-Ω coaxial line is applied with its central conductor and grounding sheath connected to Point A and B, respectively (see Fig. 2).

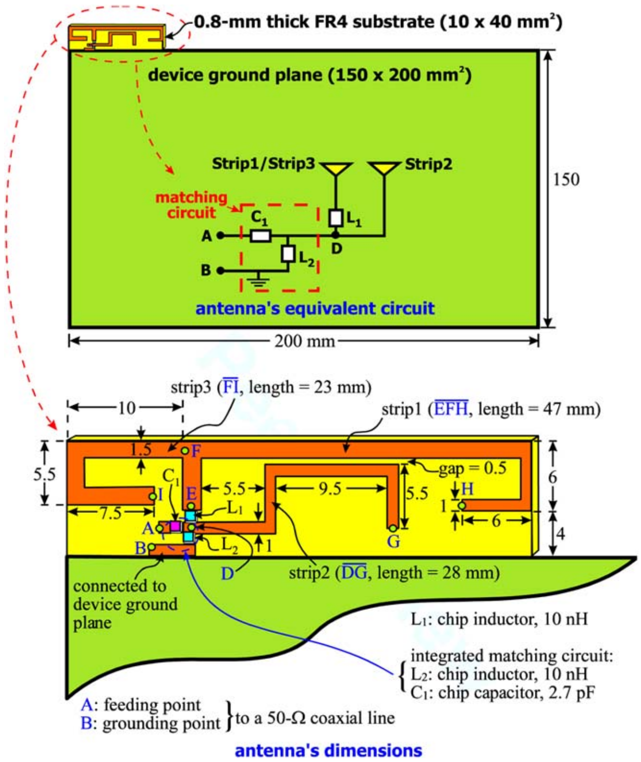

Figure 1 Geometry of the proposed LTE/WWAN/WLAN tablet computer antenna. [Color figure can be viewed in the online issue, which is available at wileyonlinelibrary.com]

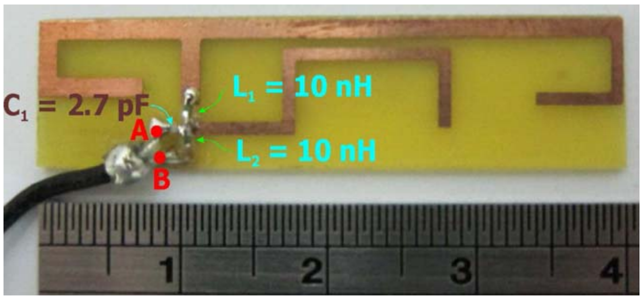

Figure 2 Photo of the fabricated antenna. [Color figure can be viewed in the online issue, which is available at wileyonlinelibrary.com]

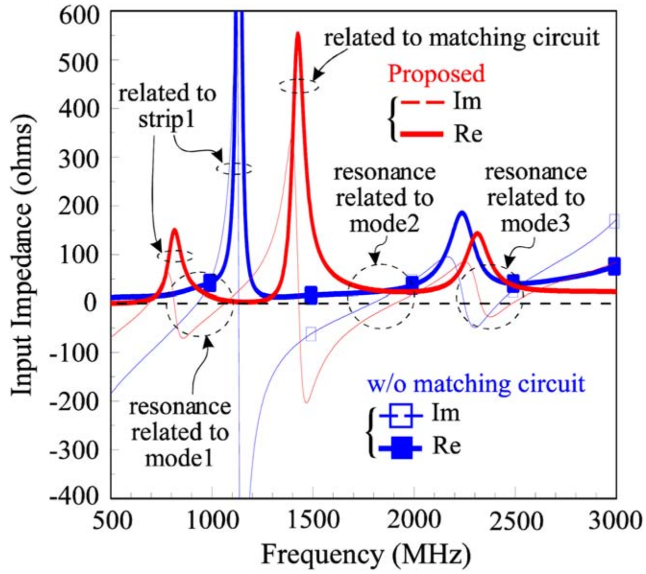

Figure 4 Simulated input impedance for the proposed antenna and the case without the integrated matching circuit. [Color figure can be viewed in the online issue, which is available at wileyonlinelibrary.com]

The antenna comprises three monopole strips of Strip1, Strip2, and Strip3. Strip1 is the longest strip (section EFH) which has a length of 47 mm and can contribute a resonant mode at about 900 MHz with the aid of a series chip inductor of 10 nH (L_1) to decrease the required resonant length [14–16]. Additionally, by adding Strip3 (section FI, length 23 mm) to Strip1 at Point F, a resonant mode at about 2.4 GHz can be generated. For Strip2 (section DG, length 28 mm), it can contribute a resonant mode at about 1900 MHz. It should be noted that in the proposed design, Strip2 is disposed between Strip1 and the edge of the device ground plane, and Strip3 is connected to Strip1 at Point F and extended in the different direction from that of Strip1 and Strip2. In addition, all the open ends of the three strips are bent and extended toward the antenna's interior or toward the edge of the device ground plane such that compact structure of the proposed antenna is obtained. Further, this arrangement can decrease possible coupling of the proposed antenna with nearby antennas or elements, which will be attractive for the proposed antenna for practical applications.

The antenna's higher band is formed by two resonant modes at about 1900 and 2400 MHz contributed by Strip2 and Strip3, respectively. In the proposed design, it is easy to adjust the resonant frequencies of the two resonant modes, simply by tuning the lengths of Strip2 and Strip3. Further, the antenna's higher band not only has a bandwidth of larger than 1 GHz to cover the frequency ranges of 1710–2170/2300–2400/2500–2690 MHz for the GSM1800/1900/UMTS/LTE2300/2500 operation, it can also have good radiation characteristics in the frequency range of 2400–2484 MHz for the 2.4-GHz WLAN operation. Simply by tuning the length of Strip3, the resonant mode covering the 2.4-GHz WLAN band can be easily adjusted.

For the antenna's lower band, although there is a resonant mode contributed by Strip1, the provided bandwidth is not

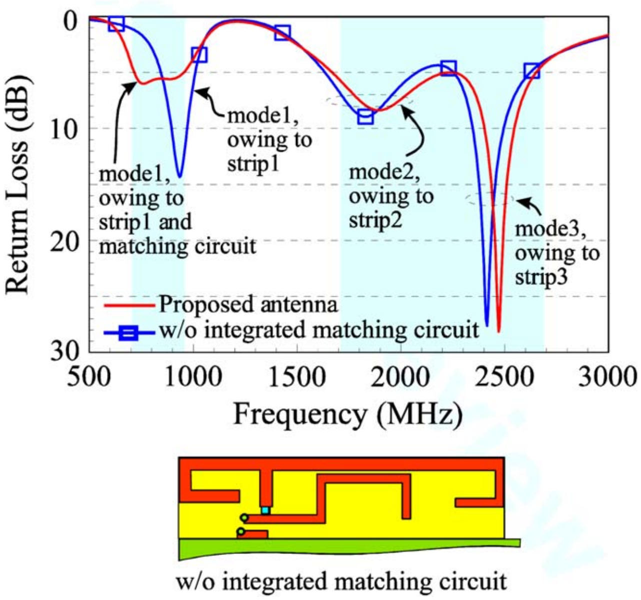

Figure 3 Simulated return loss for the proposed antenna and the case without the integrated matching circuit. [Color figure can be viewed in the online issue, which is available at wileyonlinelibrary.com]

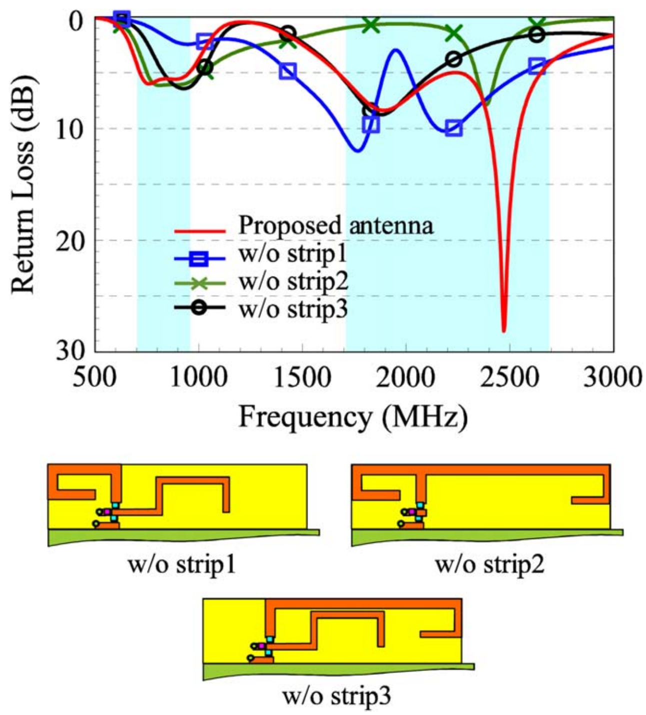

Figure 5 Simulated return loss for the proposed antenna, the case without Strip1, the case without Strip2, and the case without Strip3. [Color figure can be viewed in the online issue, which is available at wileyonlinelibrary.com]

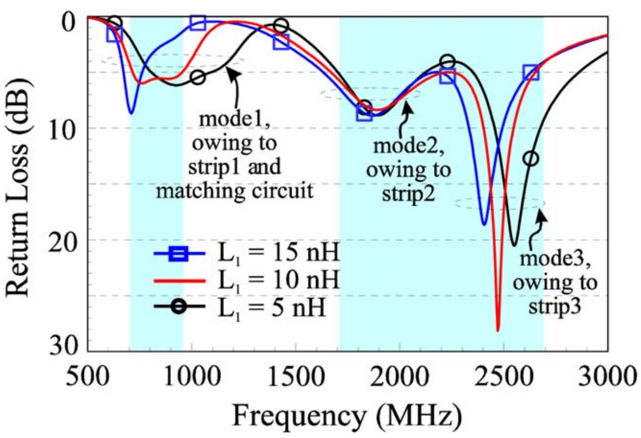

Figure 6 Simulated return loss as a function of the chip inductor L_1. [Color figure can be viewed in the online issue, which is available at wileyonlinelibrary.com]

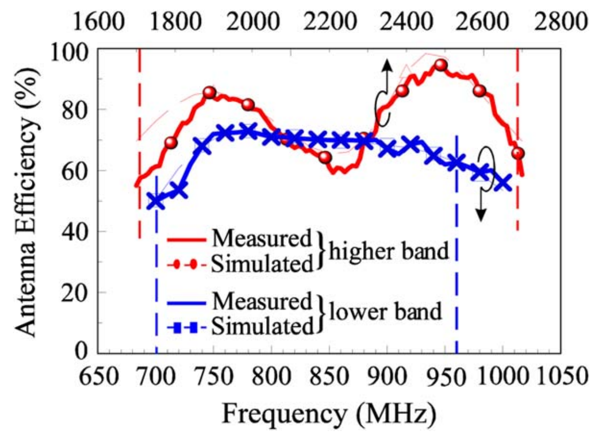

Figure 8 Measured and simulated antenna efficiency (matching loss included) of the fabricated antenna. [Color figure can be viewed in the online issue, which is available at wileyonlinelibrary.com]

enough to cover the frequency range of 704–960 MHz for the LTE700/GSM850/900 operation. To achieve a wider low-band bandwidth, a high-pass matching circuit [17] is integrated to the antenna and generally does not increase the occupied size of the antenna. The matching circuit comprises a parallel chip inductor L_2 of 10 nH and a series chip capacitor C_1 of 2.7 pF. The integrated high-pass matching circuit greatly widens the antenna's low-band bandwidth. Results of the simulated return loss for the proposed antenna and the case without the integrated matching circuit are presented in Figure 3 for comparison. The shaded frequency ranges at lower and higher frequencies in the figure represent the desired frequency ranges of 704–960 and 1710–2690 MHz. The simulated results are obtained using the EM field simulator HFSS version 14 [18]. The results show that the antenna's low-band bandwidth is greatly enhanced with the presence of the matching circuit. Conversely, the antenna's higher band formed by two resonant modes contributed by Strip2 and Strip3 is very slightly affected. It is also seen that the second mode in the higher band occurs at about 2.4 GHz, which can lead to good coverage of the 2.4-GHz WLAN operation in the frequency range of 2400–2484 MHz. Also note that although the return loss for part of the frequencies in the antenna's operating bands is not better than 6 dB, the measured antenna efficiency is all better than 50% (see Fig. 8 in Section 3) and is acceptable for practical mobile communication applications [19,20].

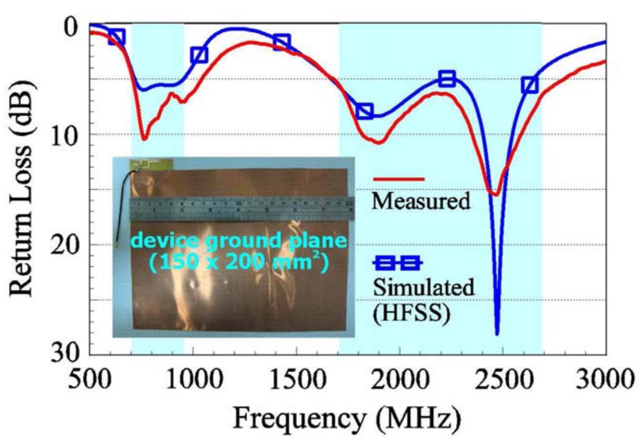

Figure 7 Measured and simulated return loss of the fabricated antenna. [Color figure can be viewed in the online issue, which is available at wileyonlinelibrary.com]

The corresponding results of the simulated input impedance for the proposed antenna and the case without the integrated matching circuit are also shown in Figure 4. It can be seen that owing to the added matching circuit, a parallel resonance [21] is generated at about 1.4 GHz and the resonant mode owing to Strip1 is shifted to lower frequencies at about 800 MHz. The generated parallel resonance greatly improves the impedance matching of the high-frequency portion of the resonant mode related to Strip1, thereby leading to a greatly widened bandwidth of the antenna's lower band as seen in Figure 3. Hence, the lower band can cover the desired LTE700/GSM850/900 operation.

To analyze the respective effects of the three strips, Figure 5 shows the simulated return loss for the proposed antenna, the case without Strip1, the case without Strip2, and the case without Strip3. When Strip1 is not present, the desired resonant mode in the antenna's lower band is not excited, while the two resonant modes in the higher band are still present. This indicates that the antenna's lower band is related to Strip1. For the case without Strip2, the first mode in the antenna's higher band disappears, while the resonant mode in the lower band and the second mode in the higher band are present. For the case without Strip3, the second mode in the higher band disappears, whereas the other two modes are present. The results indicate that Strip2 and Strip3 mainly control the first and second modes in the higher band.

Figure 6 shows the simulated return loss for the proposed antenna as a function of the chip inductor L_1. Results for L_1 varied from 5 to 15 nH are presented. Relatively smaller effects on the first mode at about 1900 MHz in the higher band are seen, and the resonant mode in the lower band and the second mode in the higher band are both shifted to higher frequencies with a decrease in the inductance of L_1. This is reasonable as in the proposed design, the chip inductor L_1 is used for achieving decreased resonant lengths of Strip1 and Strip3 only. In this case, a compact structure of the proposed antenna is obtained.

3. EXPERIMENTAL RESULTS AND DISCUSSION

Figure 7 shows the measured and simulated return loss of the fabricated antenna. The measured data agree with the simulated results. The antenna can cover the frequency bands of the LTE/WWAN and 2.4-GHz WLAN operation. Figure 8 shows the

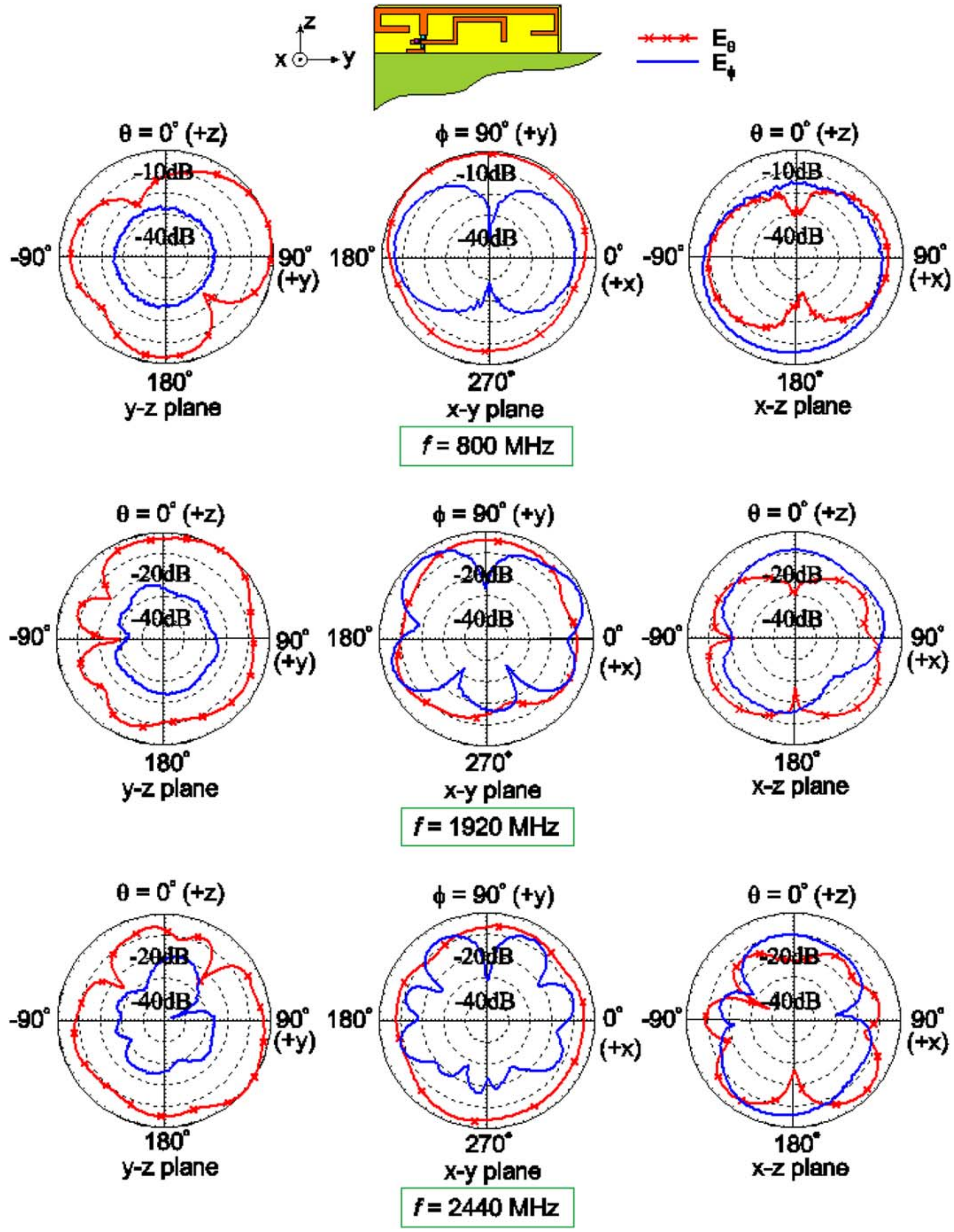

Figure 9 Measured radiation patterns of the fabricated antenna. [Color figure can be viewed in the online issue, which is available at wileyonlinelibrary.com]

measured and simulated antenna efficiency of the fabricated antenna. The antenna efficiency includes the return loss of the antenna, and agreement between the measurement and simulation is also seen. For the lower band (704–960 MHz), the measured antenna efficiency is about 50–72%. For the higher band (1710–2690 MHz), the measured antenna efficiency is about 55–94%. Note that in the 2.4-GHz WLAN band (2400–2484 MHz), enhanced antenna efficiency is obtained, and the measured antenna efficiency is better than 88%. The obtained antenna efficiency is acceptable for practical LTE/WWAN and WLAN operation.

Figure 9 shows the measured radiation patterns at representative frequencies of 800, 1920, and 2440 MHz. Radiation patterns of the principal planes (*x-y*, *x-z*, and *y-z* planes) are shown. At each frequency, the radiation intensities in the three principal planes are all normalized to the same maximum intensity. At lower frequencies (800 MHz), the antenna has an E_θ (vertical field) near-omnidirectional radiation in the azimuthal direction of the *x-y* plane pattern. At higher frequencies (1920 and 2440 MHz), small variations in the E_θ radiation in the azimuthal direction of the *x-y* plane pattern are also seen. The radiation characteristics are advantageous for mobile communications to have good coverage in practical applications.

4. CONCLUSION

A low-profile, small-size multibranch monopole antenna with integrated matching circuit for the LTE/WWAN/WLAN operation in the tablet computer has been proposed. The antenna has a planar compact structure of size 10×40 mm^2 and is easy to be disposed on one surface of a thin FR4 substrate. The antenna has been shown to provide acceptable radiation characteristics for the LTE700/GSM850/900 operation in the lower band and the GSM1800/1900/UMTS/LTE2300/2500 and 2.4-GHz WLAN operation in the higher band. The antenna is hence promising for the LTE/WWAN/WLAN operation in the slim tablet computers and is also promising to be applied in the antenna systems for the LTE MIMO, WLAN MIMO, and diversity operation owing to its small-antenna size.

REFERENCES

1. D.L. Huang, H.L. Kuo, C.F. Yang, C.L. Liao, and S.T. Lin, Compact multibranch inverted-F antenna to be embedded in a laptop computer for LTE/WWAN/IMT-E Applications, IEEE Antennas Wireless Propag Lett 9 (2010), 838–841.
2. K.L. Wong, T.W. Kang, and M.F. Tu, Internal mobile phone antenna array for LTE/WWAN and LTE MIMO operations, Microwave Opt Technol Lett 53 (2011), 1569–1573.
3. K.L. Wong, Y.C. Liu, and L.C. Chou, Bandwidth enhancement of WWAN/LTE tablet computer antenna using embedded parallel resonant circuit, Microwave Opt Technol Lett 54 (2012), 305–309.
4. T.W. Kang and K.L. Wong, Simple two-strip monopole with a parasitic shorted strip for internal eight-band LTE/WWAN laptop computer antenna, Microwave Opt Technol Lett 53 (2011), 706–712.
5. T.W. Kang, K.L. Wong, L.C. Chou, and M.R. Hsu, Coupled-fed shorted monopole with a radiating feed structure for eight-band LTE/WWAN operation in the laptop computer, IEEE Trans Antennas Propag 59 (2011), 674–679.
6. Y.L. Ban, S.C. Sun, J.L.W. Li, and W. Hu, Compact coupled-fed wideband antenna for internal eight-band LTE/WWAN tablet computer applications, J Electromagn Waves Appl 26 (2012), 2222–2233.
7. S.H. Chang and W.J. Liao, A broadband LTE/WWAN antenna design for tablet PC, IEEE Trans Antennas Propag 60 (2012), 4354–4359.
8. J.H. Lu and Y.S. Wang, Internal uniplanar antenna for LTE/GSM/UMTS operation in a tablet computer, IEEE Trans Antennas Propag 61 (2013), 2841–2846.
9. K.L. Wong, H.J. Jiang, and T.W. Weng, Small-size planar LTE/WWAN antenna and antenna array formed by the same for tablet computer application, Microwave Opt Technol Lett 55 (2013), 1928–1934.
10. K.L. Wong and W.J. Lin, WWAN/LTE printed slot antenna for tablet computer application, Microwave Opt Technol Lett 54 (2012), 44–49.
11. T.W. Kang and K.L. Wong, Internal printed loop/monopole combo antenna for LTE/GSM/UMTS operation in the laptop computer, Microwave Opt Technol Lett 52 (2010), 1673–1678.
12. K.L. Wong and T.J. Wu, Small-size LTE/WWAN coupled-fed loop antenna with band-stop matching circuit for tablet computer, Microwave Opt Technol Lett 54 (2012), 1189–1193.
13. K.L. Wong, W.J. Wei, L.C. Chou, WWAN/LTE printed loop antenna for tablet computer and its body SAR analysis, Microwave Opt Technol Lett 53 (2011), 2912–1919.
14. K.L. Wong and S.C. Chen, Printed single-strip monopole using a chip inductor for pentaband WWAN operation in the mobile phone, IEEE Trans Antennas Propag 58 (2010), 1011–1014.
15. T.W. Kang and K.L. Wong, Chip-inductor-embedded small-size printed strip monopole for WWAN operation in the mobile phone, Microwave Opt Technol Lett 51 (2009), 966–971.
16. J. Thaysen and K.B. Jakobsen, A size reduction technique for mobile phone PIFA antennas using lumped inductors, Microwave J 48 (2005), 114–126.
17. K.L. Wong and T.W. Kang, GSM850/900/1800/1900/UMTS printed monopole antenna for mobile phone application, Microwave Opt Technol Lett 50 (2008), 3192–3198.
18. Available at: http://www.ansys.com/products/, ANSYS HFSS, Pittsburgh, PA.
19. C.H. Li, E. Ofli, N. Chavannes, and N. Kuster, Effects of hand phantom on mobile phone antenna performance, IEEE Trans Antennas Propag 57 (2009), 2763–2770.
20. C.L. Liu, Y.F. Lin, C.M. Liang, S.C. Pan, and H.M. Chen, Miniature internal penta-band monopole antenna for mobile phones, IEEE Trans Antennas Propag 58 (2010), 1008–1011.
21. K.L. Wong, Y.W. Chang, and S.C. Chen, Bandwidth enhancement of small-size WWAN tablet computer antenna using a parallel-resonant spiral slit, IEEE Trans Antennas Propag 60 (2012), 1705–1711.

A WAVELENGTH SPACING SWITCHABLE AND TUNABLE HIGH-BIREFRINGENCE FIBER LOOP MIRROR FILTER

Si-Yuan Bian,[1,2] Mei-Qi Ren,[1,2] and Li Wei[1,2]

[1] Department of Physics and Computer Science, Wilfrid Laurier University, Waterloo, ON, Canada N2L 3C5; Corresponding author: lwei@wlu.ca

[2] Department of Physics and Astronomy, Guelph-Waterloo Physics Institute, University of Waterloo, Waterloo, ON, Canada N2L 3G1

Received 16 October 2013

ABSTRACT: *We demonstrated an all-fiber birefringent comb filter with tunable and switchable wavelength spacing. The comb filter is based on a fiber loop mirror (FLM) with three sections of high-birefringence (HB) fibers and polarization controllers (PCs). The transmission characteristics of the birefringent FLM are dependent of the relative phase difference of the two orthogonal polarization modes and the rotational angles of the different HB fibers. By adjusting the PCs, four different wavelength spacings can be obtained; particularly, interleaving operation—halved and quartered wavelength spacing—can be effectively realized. By using a Jones matrix method, the transmission of the birefringent comb filter is analyzed. The theoretical analysis agrees with the experimental results.* © 2014 Wiley Periodicals, Inc. Microwave Opt Technol Lett 56:1666–1670, 2014; View this article online at wileyonlinelibrary.com. DOI 10.1002/mop.28415

Key words: *comb filter; fiber loop mirror; wavelength spacing tunable; polarization-maintaining fiber*

1. INTRODUCTION

Fiber loop mirrors (FLMs) are extremely important building blocks for applications in fiber-optic sensing technology and dense wavelength-division-multiplexing (DWDM) network systems. By simply connecting the two output ports of a 3-dB coupler, a basic FLM is constructed. The two waves split at input end prorogate in opposite directions with the same optical phase difference, resulting in a constructive interference at the input end. In general, a FLM is considered as a perfect reflector (assuming the loss is negligible). By inserting a polarization controller (PC) to introduce a small controllable birefringence in the loop, such a basic FLM becomes an all-fiber mirror with a variable reflectivity [1,2]. Furthermore, by introducing a high-birefringence (HB) fiber inside the loop, the specific birefringent FLM could turn into an all-fiber interferometer [3–12], which can be used as an optical comb filter in generating multiwavelength laser sources [4–6], processing microwave and optical signals [7], optical networks [8], flattening optical gain [9], measuring birefringence [10], capturing environmental parameters [11,12] and so on.

To enhance the operational flexibility and functionality of the devices in configurable and dynamic environment, the tunability